

## THE CRYSTAL STRUCTURE OF FAHEYITE, $\text{Mn}^{2+}\text{Fe}^{3+}_2[\text{Be}_2(\text{PO}_4)_4](\text{H}_2\text{O})_6$ : A NEW TWIST FOR THE $[\text{Be}(\text{P}\Phi_4)_2]$ CHAIN

MARK A. COOPER AND FRANK C. HAWTHORNE<sup>§</sup>

*Department of Geological Sciences, University of Manitoba, 125 Dysart Road, Winnipeg, Manitoba, R3T 2N2 Canada*

### ABSTRACT

The crystal structure of faheyite, ideally  $\text{Mn}^{2+}\text{Fe}^{3+}_2[\text{Be}_2(\text{PO}_4)_4](\text{H}_2\text{O})_6$ , trigonal,  $a$  9.404(7),  $c$  15.920(11) Å,  $V$  1219(2) Å<sup>3</sup>,  $Z = 3$ , space group  $P3_121$ , has been solved and refined to an  $R_1$  index of 4.4% with single-crystal X-ray diffraction data collected from a twinned fiber. There are two  $P$  sites that are tetrahedrally coordinated by O atoms with  $\langle P\text{-O} \rangle$  distances of 1.52 and 1.54 Å, respectively, one  $Be$  site tetrahedrally coordinated by O atoms with a  $\langle Be\text{-O} \rangle$  distance of 1.63 Å, one  $Mn$  site occupied by  $\text{Mn}^{2+}$  coordinated by four O atoms and two (H<sub>2</sub>O) groups with a  $\langle Mn\text{-O} \rangle$  distance of 2.22 Å, and one  $Fe$  site occupied by  $\text{Fe}^{3+}$  coordinated by four O atoms and two (H<sub>2</sub>O) groups with a  $\langle Fe\text{-O} \rangle$  distance of 2.01 Å.

Each vertex of the  $Be$  tetrahedron is shared with a vertex of a neighboring  $P$  tetrahedron, and two vertices of each  $P$  tetrahedron are shared with neighboring  $Be$  tetrahedra to form a corner-sharing  $[\text{Be}(\text{PO}_4)_2]$  chain, with  $P$  tetrahedra flanking the  $Be$  tetrahedra of the central spine in the sequence  $-P(1)/P(1)\text{-}Be\text{-}P(2)/P(2)\text{-}Be\text{-}$ . Faheyite has a chiral structure, with the  $[\text{Be}(\text{PO}_4)_2]$  chain twisting about the  $c$ -axis in a clockwise direction for the refined  $P3_121$  enantiomer. The  $Mn$  octahedron lies along the  $3_1$  screw axis within the core region of the  $[\text{Be}(\text{PO}_4)_2]$  chain, forming  $[\text{MnBe}_2(\text{PO}_4)_4]$  spires that are wrapped by  $Fe$  octahedra that share vertices with  $P$  tetrahedra. The crystal structures of fransoletite and parafransoletite also contain beryllophosphate chains topologically identical to that found in faheyite, although the  $[\text{Be}(\text{PO}_4)(\text{PO}_3\text{OH})]$  chain in fransoletite and parafransoletite is straight, whereas the  $[\text{Be}(\text{PO}_4)_2]$  chain in faheyite forms a helix about the central  $c$ -axis.

**Keywords:** faheyite, crystal structure, phosphate, transition metal, Roosevelt mine, South Dakota, U.S.A.

### INTRODUCTION

Faheyite was originally described from the Sapucaia Velha pegmatite mine, Galileia, Minas Gerais, Brazil, as a hexagonal ( $a = 9.43$ ,  $c = 16.00$  Å) beryllium-phosphate-hydrate mineral with the formula  $\text{Mn}^{2+}\text{Be}_2\text{Fe}^{3+}_2(\text{PO}_4)_4(\text{H}_2\text{O})_6$ ,  $Z = 3$  (Lindberg & Murata 1953). It is a late secondary mineral (Černý 2002) and occurs as botryoidal tufts and rosettes of white to bluish-and brownish-white fibers coating muscovite, quartz, variscite, and frondelite, and is also associated with roscherite. It has been identified from the Noumas pegmatite, Namaqualand, South Africa (von Knorring 1985), and from the Roosevelt mine near Custer, Custer County, South Dakota, U.S.A. (Robinson *et al.* 1992). Single-crystal X-ray study showed that faheyite has Laue symmetry  $6/mmm$  and systematically absent reflections that are consistent with the enantiomorphic space groups  $P6_222$  and  $P6_422$ , in crystal class 622 (Lindberg 1964). As part of our general interest in phosphate (Huminicki & Hawthorne 2002) and

beryllate minerals (Hawthorne & Huminicki 2002), we have solved the crystal structure of faheyite and present the results here.

### X-RAY DATA COLLECTION AND STRUCTURE-REFINEMENT

#### Sample

Colorless fibers of faheyite from the Roosevelt mine, South Dakota (Robinson *et al.* 1992), were provided by Roy Kristiansen.

#### Data collection

A colorless fiber of faheyite (Table 1) was attached to a tapered glass fiber and mounted on a Bruker D8 three-circle diffractometer equipped with a rotating-anode generator (MoK $\alpha$  X-radiation), multi-layer optics, and an APEX-II CCD area detector. In excess of a Ewald sphere of diffraction data was

<sup>§</sup> Corresponding author e-mail address: frank\_hawthorne@umanitoba.ca

TABLE 1. MISCELLANEOUS INFORMATION FOR FAHEYITE

<i>a</i> (Å)	9.404(7)	Crystal size (µm)	3.5 × 3.5 × 90
<i>c</i>	15.920(11)	Radiation	MoKα
<i>V</i> (Å <sup>3</sup> )	1219(2)	No. of intensities	22324
Space group	<i>P</i> 3 <sub>1</sub> 21	No. in Ewald sphere	6418
<i>Z</i>	3	No. unique reflections	1079
Twin fraction	0.469(5)	No. with ( <i>F</i> <sub>o</sub> > 4σ <i>F</i> )	942
Flack parameter	-0.09(8)	<i>R</i> <sub>merge</sub> %	7.9
		<i>R</i> <sub>1</sub>	4.4
		<i>wR</i> <sub>2</sub>	11.1

Cell content: 3[Mn<sup>2+</sup>Be<sub>2</sub>Fe<sup>3+</sup><sub>2</sub>(PO<sub>4</sub>)<sub>4</sub>(H<sub>2</sub>O)<sub>6</sub>]

$$R_1 = \frac{\sum(|F_o| - |F_c|)}{\sum|F_o|}$$

$$wR_2 = \frac{[\sum w(F_o^2 - F_c^2)^2 / \sum w(F_o^2)^2]^{1/2}}{w}, \quad w = 1/[\sigma^2(F_o^2) + (0.0693 P)^2 + 3.05 P]$$

where  $P = (\max(F_o^2, 0) + 2F_c^2)/3$

collected to 60° 2θ using 80 s frames, a 0.2° frame width, and a crystal-to-detector distance of 5 cm. There was no observable X-ray diffraction intensity from 45 to 60° 2θ, and the raw data frames were integrated with a resolution limit of 0.93 Å (corresponding to 45° 2θ), giving a total of 22,324 reflections. Empirical absorption corrections (SADABS, Sheldrick 2008) were applied and equivalent reflections were corrected for Lorentz, polarization, and background effects, and averaged and reduced to structure factors, resulting in 6418 individual reflections within the Ewald sphere. The unit-cell dimensions were obtained by least-squares refinement of the positions of 3691 reflections with  $I > 7\sigma I$  and are given in Table 1, together with other information pertaining to data collection and structure refinement.

#### Structure solution and refinement

All calculations were done with the SHELXTL PC (Plus) system of programs (Bruker 1997); *R* indices are of the form given in Table 1 and are expressed as percentages. Following the results of Lindberg (1964), we first attempted to solve the faheyite structure in the space groups *P*6<sub>2</sub>22 and *P*6<sub>4</sub>22, which proved unsuccessful. A rudimentary complete structure corresponding to the earlier proposed formula was solved and refined in *P*1; however, the high *R* value (13%) indicated there were underlying issues that would need addressing. Analysis of the *P*1 atom arrangement using the MISSYM program (LePage 1988) indicated that the space group *P*3<sub>1</sub>21 is conformable with the diffraction data, and this was confirmed by subsequent refinement in *P*3<sub>1</sub>21. However, the *R* value remained at 13%. In the *P*1 and *P*3<sub>1</sub>21 models, the electron-scattering centers were at the same relative positions, and the discrepancy between the intensity data and each refinement model was independent of the differing space-group symmetry.

The *P*3<sub>1</sub>21 refinement had the following characteristics: (1) nearly all sites had atomic-displacement

parameters that were non-positive-definite for an anisotropic-displacement model; (2) nearly all of the worst-fit reflections had  $|F_o| > |F_c|$ ; (3) the *E*-statistic for the data was notably low at 0.675; (4) the *R*<sub>merge</sub> value for the higher-symmetry Laue group 6/*mmm* (6.1%) is only slightly higher than for the lower-symmetry Laue group 3̄*m*1 (5.3%). This combination of characteristics is a well-known indication of possible twinning, and the two classic twin laws commonly exhibited by quartz (Dauphine, Brazil) were investigated, as both quartz and faheyite crystallize in the same space group. We found a distinctive improvement in *R* value for both an isotropic-displacement model (6.6%) and an anisotropic-displacement model (3.6%) incorporating a variable Dauphine-style twin component (*i.e.*, 2-fold rotation twin-axis parallel to [001]; 0.469 twin fraction). Although the *R* value of 3.6% for the anisotropic-displacement model was significantly lower than the *R* value of 6.6% for the isotropic-displacement model, nearly all atoms had non-positive-definite anisotropic-displacement parameters, and the refinement showed convergence problems. To help alleviate this problem (twinning adversely affecting anisotropic modeling of the atom displacements), we introduced displacement-parameter constraints that allowed sensible anisotropic-displacement parameters and (in turn) proper refinement convergence. We then compared all individual bond lengths between the displacement-restrained (anisotropic) and unrestrained (isotropic) models and noted slightly less overall dispersion in Be–O and P–O bond lengths for the displacement-restrained (anisotropic) model: the Be–O and P–O distances for the unrestrained (isotropic) model spanned 1.53–1.69 and 1.46–1.57 Å, respectively, whereas the analogous distances for the displacement-restrained (anisotropic) model ranged from 1.59–1.68 and 1.48–1.56 Å, respectively. The Flack parameter refined to -0.09(8) and confirmed the correct absolute structure, but we were unable to locate the H positions in the final difference-Fourier map.

TABLE 2. ATOM COORDINATES AND ANISOTROPIC-DISPLACEMENT PARAMETERS ( $\text{\AA}^2$ ) FOR FAHEYITE

Site	<i>x</i>	<i>y</i>	<i>z</i>	$U_{11}$	$U_{22}$	$U_{33}$	$U_{23}$	$U_{13}$	$U_{12}$	$U_{\text{eq}}$
<i>Be</i>	0.844(8)	0.6861(17)	0.084(2)	0.016(3)	0.016(3)	0.016(3)	0.0000(11)	-0.0001(11)	0.0080(18)	0.016(3)
<i>P</i> (1)	0.6093(13)	0.7910(15)	0.0909(3)	0.017(2)	0.018(2)	0.010(2)	0.0002(10)	0.0006(10)	0.0069(13)	0.0155(18)
<i>P</i> (2)	0.1799(13)	0.7922(13)	0.0815(3)	0.0117(19)	0.0122(19)	0.0045(19)	-0.0013(9)	0.0001(9)	0.0041(12)	0.0103(17)
<i>Fe</i>	0.5536(10)	0.1078(2)	0.0826(2)	0.0176(9)	0.0205(8)	0.0038(7)	0.0003(8)	0.0007(7)	0.0067(9)	0.0152(4)
<i>Mn</i>	0	-0.0012(4)	1/6	0.0235(10)	0.0246(9)	0.0169(9)	-0.0007(4)	-0.0013(9)	0.0118(5)	0.0218(6)
O(1)	0.7815(19)	0.8167(19)	0.1013(9)	0.014(3)	0.014(3)	0.013(3)	0.0001(11)	0.0003(11)	0.0069(17)	0.014(3)
O(2)	0.493(2)	0.638(2)	0.1357(9)	0.021(3)	0.021(3)	0.020(3)	0.0004(11)	0.0003(11)	0.0102(19)	0.021(3)
O(3)	0.608(2)	0.9465(19)	0.1226(10)	0.021(4)	0.021(3)	0.019(4)	0.0002(11)	-0.0005(11)	0.010(2)	0.020(3)
O(4)	0.5704(14)	0.7657(19)	-0.0016(12)	0.018(3)	0.018(3)	0.016(3)	-0.0002(11)	0.0001(11)	0.0083(16)	0.017(3)
O(5)	0.1993(17)	0.7619(18)	0.1726(11)	0.011(3)	0.011(3)	0.009(3)	-0.0002(11)	0.0003(11)	0.0053(16)	0.011(3)
O(6)	0.143(2)	0.636(2)	0.0306(9)	0.015(3)	0.015(3)	0.014(3)	-0.0005(11)	0.0002(11)	0.0068(17)	0.015(3)
O(7)	0.3337(19)	0.9412(17)	0.0444(9)	0.010(3)	0.011(3)	0.009(3)	0.0003(11)	-0.0003(11)	0.0045(17)	0.010(3)
O(8)	0.041(2)	0.834(2)	0.0710(10)	0.016(3)	0.016(3)	0.015(3)	-0.0004(11)	0.0002(11)	0.0074(19)	0.016(3)
O(9)	0.799(2)	0.292(2)	0.1167(10)	0.023(4)	0.023(4)	0.022(4)	-0.0001(11)	-0.0004(11)	0.011(2)	0.023(4)
O(10)	0.492(2)	0.2894(19)	0.0500(10)	0.019(3)	0.019(3)	0.018(4)	0.017(4)	0.0003(11)	-0.0003(11)	0.009(2)
O(11)	0.097(3)	0.2144(13)	0.0893(13)	0.040(3)	0.040(3)	0.040(3)	0.0004(11)	0.0000(11)	0.0197(17)	0.040(3)

TABLE 3. SELECTED INTERATOMIC DISTANCES (Å) AND ANGLES (°) IN FAHEYITE

<i>Be</i> -O(1)	1.63(6)	<i>P</i> (1)-O(1)	1.52(2)	
<i>Be</i> -O(4)	1.63(4)	<i>P</i> (1)-O(2)	1.48(2)	
<i>Be</i> -O(5)	1.59(4)	<i>P</i> (1)-O(3)	1.55(2)	
<i>Be</i> -O(8)	1.68(6)	<i>P</i> (1)-O(4)	1.51(2)	
< <i>Be</i> -O>	1.63	< <i>P</i> (1)-O>	1.52	
<i>Fe</i> -O(2)	1.96(2)	<i>P</i> (2)-O(5)	1.51(2)	
<i>Fe</i> -O(3)	1.93(2)	<i>P</i> (2)-O(6)	1.55(2)	
<i>Fe</i> -O(6)	1.92(2)	<i>P</i> (2)-O(7)	1.54(2)	
<i>Fe</i> -O(7)	1.96(2)	<i>P</i> (2)-O(8)	1.56(2)	
<i>Fe</i> -O(9)	2.15(2)	< <i>P</i> (2)-O>	1.54	
<i>Fe</i> -O(10)	2.12(2)			
< <i>Fe</i> -O>	2.01	<i>Mn</i> -O(1)	2.17(2)	×2
$\Delta_{\text{oct}} \times 10^3$	1.94	<i>Mn</i> -O(8)	2.33(2)	×2
		<i>Mn</i> -O(11)	2.15(2)	×2
O(6)- <i>Fe</i> -O(9)	85.3(7)	< <i>Mn</i> -O>	2.22	
O(6)- <i>Fe</i> -O(10)	83.2(6)	$\Delta_{\text{oct}} \times 10^3$	1.32	
O(6)- <i>Fe</i> -O(7)	91.2(7)			
O(6)- <i>Fe</i> -O(3)	101.6(7)	O(1)- <i>Mn</i> -O(8)	64.5(4)	×2
O(9)- <i>Fe</i> -O(10)	91.5(3)	O(1)- <i>Mn</i> -O(8)	87.8(7)	×2
O(10)- <i>Fe</i> -O(7)	88.0(7)	O(1)- <i>Mn</i> -O(11)	104.9(7)	×2
O(7)- <i>Fe</i> -O(3)	93.6(3)	O(1)- <i>Mn</i> -O(11)	101.8(8)	×2
O(3)- <i>Fe</i> -O(9)	87.2(7)	O(8)- <i>Mn</i> -O(11)	96.8(6)	×2
O(2)- <i>Fe</i> -O(9)	82.2(7)	O(8)- <i>Mn</i> -O(8)	83.8(9)	
O(2)- <i>Fe</i> -O(10)	84.8(7)	O(11)- <i>Mn</i> -O(11)	86.0(1.2)	
O(2)- <i>Fe</i> -O(7)	101.1(7)	<O- <i>Mn</i> -O>	90.12	
O(2)- <i>Fe</i> -O(3)	90.2(8)	$\sigma_{\text{oct}}^2$	198.1	
<O- <i>Fe</i> -O>	89.99			
$\sigma_{\text{oct}}^2$	40.2			
Possible H-bonding				
O(9)-O(5)	2.63(2)	O(11)-O(3)	3.11(3)	
O(9)-O(7)	2.83(2)	O(11)-O(10)	3.22(2)	
O(5)-O(9)-O(7)	109.6(7)	O(3)-O(11)-O(10)	94.7(6)	
O(10)-O(3)	2.84(2)	O(11)-O(7)	3.08(2)	
O(10)-O(4)	2.72(2)	O(11)-O(9)	3.05(2)	
O(3)-O(10)-O(4)	108.9(7)	O(7)-O(11)-O(9)	99.2(6)	

We regard the well-converged displacement-restrained (anisotropic) model (final  $R = 4.4\%$ ) as the optimal structure representation. Final atom coordinates for this model are given in Table 2, selected interatomic distances and angles in Table 3, and bond valences, calculated with the parameters of Brown & Altermatt (1985), in Table 4. A table of structure-factors and a cif file may be obtained from The Depository of Unpublished Data on the MAC website [document faheyite CM53-2\_10.3749/canmin.1400049].

## DESCRIPTION OF THE STRUCTURE

In the following discussion, cation sites are italicized, and coordination polyhedra are labelled by their central site.

TABLE 4. BOND-VALENCE VALUES\* FOR FAHEYITE

	<i>Be</i>	<i>P</i> (1)	<i>P</i> (2)	<i>Fe</i>	<i>Mn</i>	$\Sigma$
O(1)	0.51	1.30			0.36 <sup>x2</sup> ↓	2.17
O(2)		1.45		0.58		2.03
O(3)		1.20		0.63		1.83
O(4)	0.51	1.34				1.85
O(5)	0.57		1.34			1.91
O(6)			1.20	0.65		1.85
O(7)			1.23	0.58		1.81
O(8)	0.45		1.17		0.23 <sup>x2</sup> ↓	1.85
O(9)				0.35		0.35
O(10)				0.38		0.38
O(11)					0.38 <sup>x2</sup> ↓	0.38
$\Sigma$	2.04	5.29	4.94	3.17	1.94	

\*From Brown & Altermatt (1985)

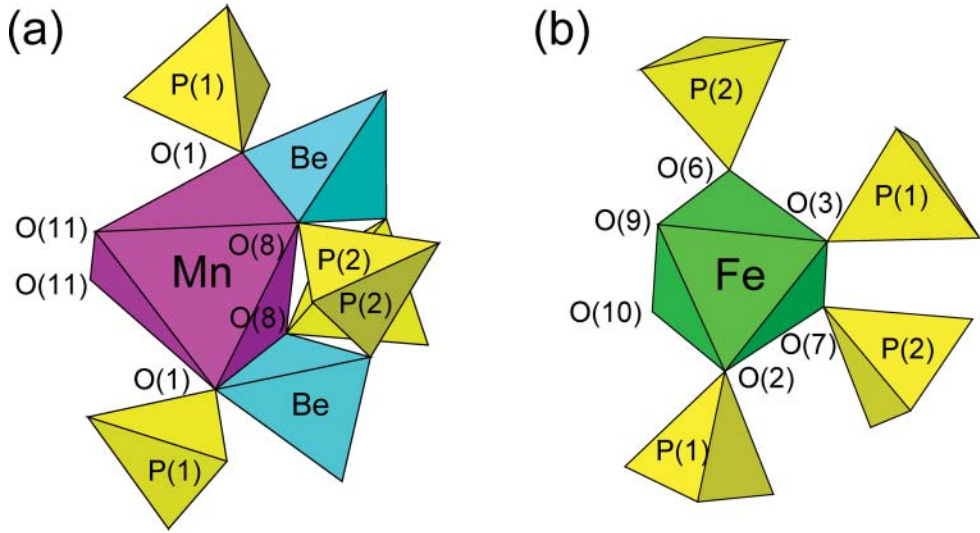


FIG. 1. The octahedral environments in faheyite: (a) *Mn* octahedron; (b) *Fe* octahedron; O(9), O(10), and O(11) are (H<sub>2</sub>O) groups.

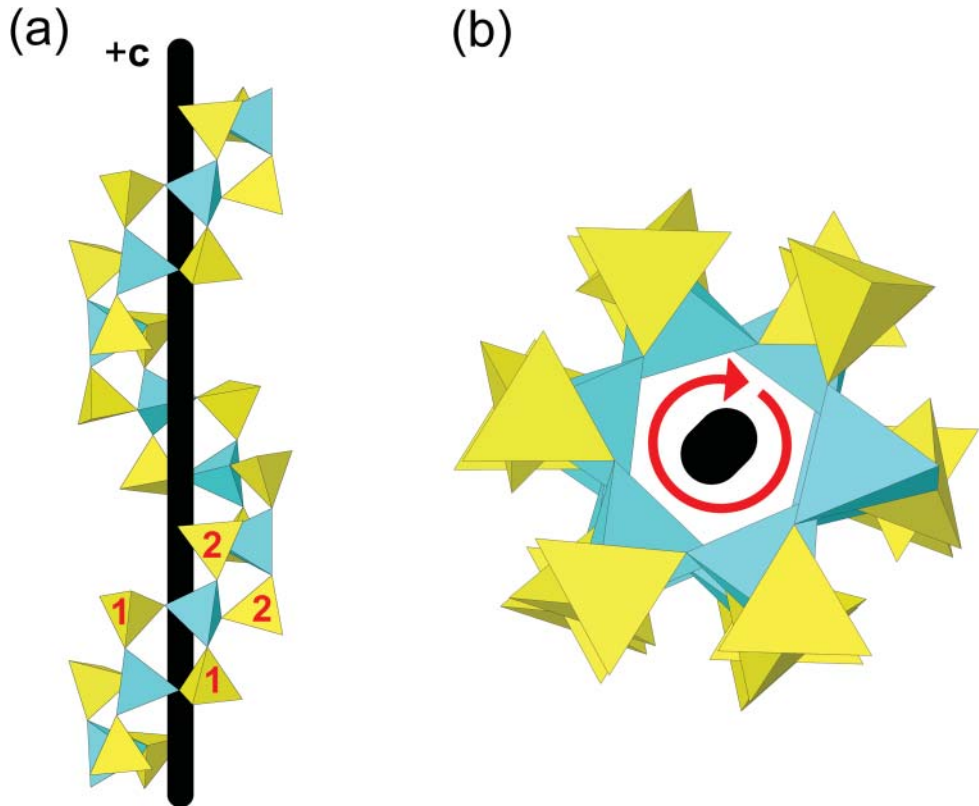


FIG. 2. The  $[\text{Be}(\text{PO}_4)_2]$  chain in faheyite (a) projected down an axis  $10^\circ$  from  $[100]$  with  $[001]$  in the page plane; (b) projected down an axis slightly rotated from  $[001]$ . *Be* tetrahedra: blue shading; *P* tetrahedra: yellow shading; red numbers: *P* atom designators; red arrow: denotes clockwise chain rotation.

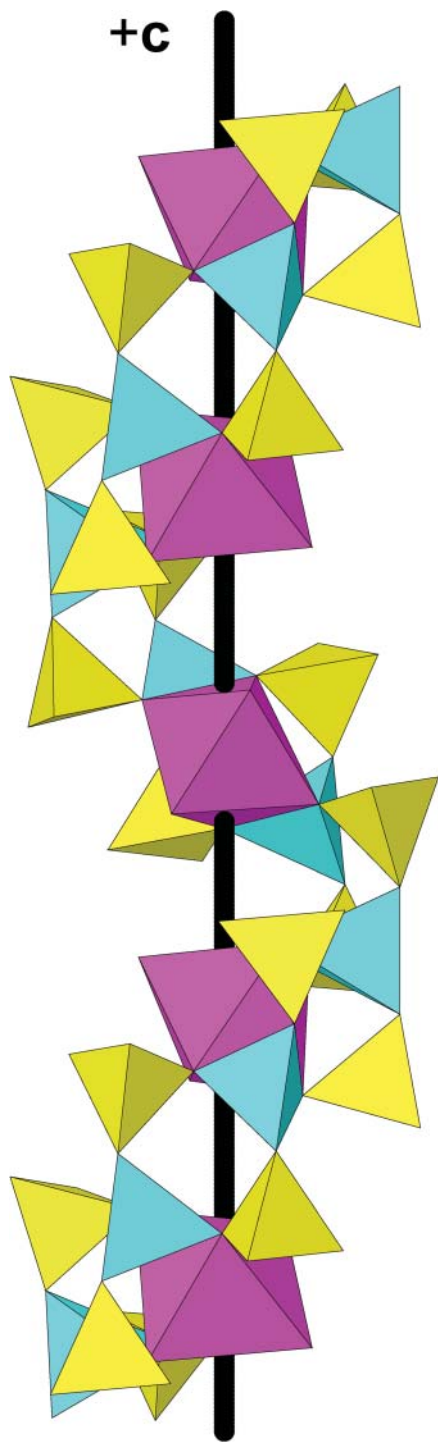


FIG. 3. The  $\text{MnBe}_2(\text{PO}_4)_4$  spire in faheyite, projected down an axis  $10^\circ$  from  $[100]$  with  $[001]$  in the page plane. Legend as in Figures 1, 2.

### Site occupancies

There are two  $P$  sites,  $P(1)$  and  $P(2)$ , occupied by  $\text{P}^{5+}$  that are tetrahedrally coordinated by O atoms with  $\langle P-O \rangle$  distances of 1.52 and 1.54 Å, respectively (Table 3), close to the grand  $\langle P-O \rangle$  distance in minerals of 1.537 Å given by Huminicki & Hawthorne (2002). There is one  $Be$  site, occupied by  $\text{Be}^{2+}$ , that is tetrahedrally coordinated by O atoms with a  $\langle Be-O \rangle$  distance of 1.63 Å (Table 3), close to the grand  $\langle Be-O \rangle$  distance in minerals of 1.633 Å given by Hawthorne & Huminicki (2002).

The  $Mn$  site is octahedrally coordinated by four O atoms and two ( $\text{H}_2\text{O}$ ) groups [ $\text{O}(11) = \text{H}_2\text{O}$ ] with a  $\langle Mn-O \rangle$  distance of 2.22 Å (Table 3); both the site-scattering and mean bond length are consistent with full occupancy by  $\text{Mn}^{2+}$ . The  $Fe$  site is also octahedrally coordinated by four O atoms and two ( $\text{H}_2\text{O}$ ) groups [ $\text{O}(9)$ ,  $\text{O}(10) = \text{H}_2\text{O}$ ] with a  $\langle Fe-O \rangle$  distance of 2.01 Å; both the site-scattering and mean bond length are consistent with full occupancy by  $\text{Fe}^{3+}$ . Summing the constituent cation and anion radii [from Shannon 1976, with  $r(\text{H}_2\text{O}) = 1.36$  Å] for the  $Mn$  and  $Fe$  sites:  $Mn$   $0.83 + 1.36 = 2.19$  Å,  $Fe$   $0.645 + 1.353 = 2.00$  Å, gives values very close to the observed mean bond lengths, indicating the absence of significant  $\text{Mn}^{2+}$ - $\text{Fe}^{3+}$  disorder in faheyite.

The  $\text{H}_2\text{O}$  groups are in a *cis* configuration for both octahedra (Fig. 1), with no further cation interactions involving the  $\text{H}_2\text{O}$  groups (other than H atoms). The  $Fe-O(9)$  and  $Fe-O(10)$  distances involving the two  $\text{H}_2\text{O}$  groups are significantly longer than the other four  $Fe-O$  distances (Table 3), resulting in the  $Fe$  octahedron having a greater bond-length distortion (relative to the  $Mn$  octahedron). This elongation of the  $\text{Fe}^{3+}$ -( $\text{H}_2\text{O}$ ) bond-length reduces the incident bond-valence at the  $\text{O}(9)$  and  $\text{O}(10)$  anions, which presumably is favorable in helping the O anions of the ( $\text{H}_2\text{O}$ ) groups attain their requisite incident bond-valence sums. The  $Mn$  octahedron contains a lower-valence cation ( $\text{Mn}^{2+}$ ), and there seems to be no similar driving force to lengthen the  $Mn-O(11)$  bond to the ( $\text{H}_2\text{O}$ ) group. The four O-atoms [ $\text{O}(1) \times 2$ ,  $\text{O}(8) \times 2$ ] coordinating Mn are each shared by neighboring P and Be atoms (Fig. 1a). The  $Mn$  octahedron and Be tetrahedron share an edge,  $\text{O}(1)-\text{O}(8)$ , and this shared edge is much shorter than the other edges of the  $Mn$  octahedron (*i.e.*, 2.41 versus 2.93–3.43 Å). The  $Fe$  octahedron shares each of its O vertices with neighboring P atoms only (Fig. 1b), and the edges of the  $Fe$  octahedron show much less variation (*i.e.*, 2.69–3.06 Å) than is the case for the  $Mn$  octahedron. The different linkage of the  $Mn$  and  $Fe$  octahedra to neighboring Be and P tetrahedra results in a much greater angular distortion of the  $Mn$  octahedron compared to the  $Fe$  octahedron (Table 3). There is no direct linkage between octahedra, and this spatial isolation of completely ordered transition-metal

species ( $\text{Mn}^{2+}$ ,  $\text{Fe}^{3+}$ ) explains why faheyite is nearly colorless, as any color will be caused by (spin-forbidden)  $d-d$  transitions and not IVCT (intervalence charge-transfer transitions).

#### Bond topology

Each vertex of the *Be* tetrahedron is shared with a vertex of a neighboring *P* tetrahedron, and two vertices

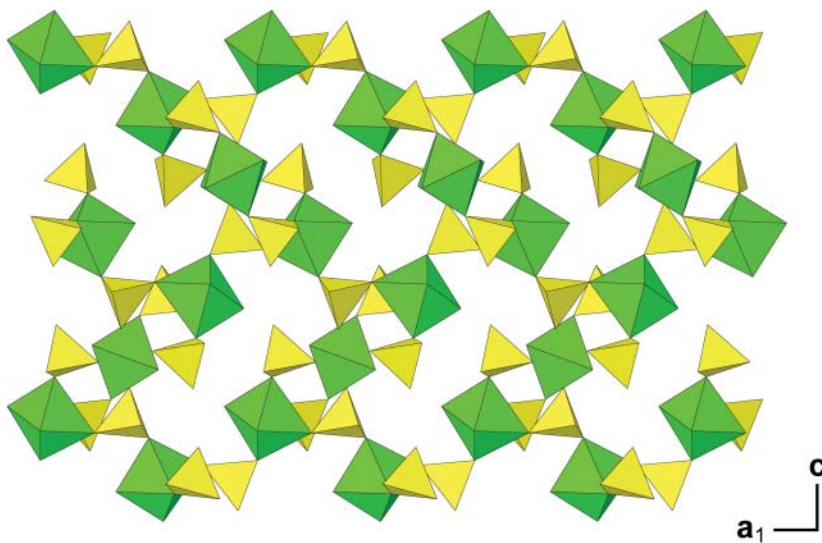


FIG. 4. The *Fe* octahedron – *P* tetrahedron connectivity in faheyite along a (010) slab. Legend as in Figure 2.

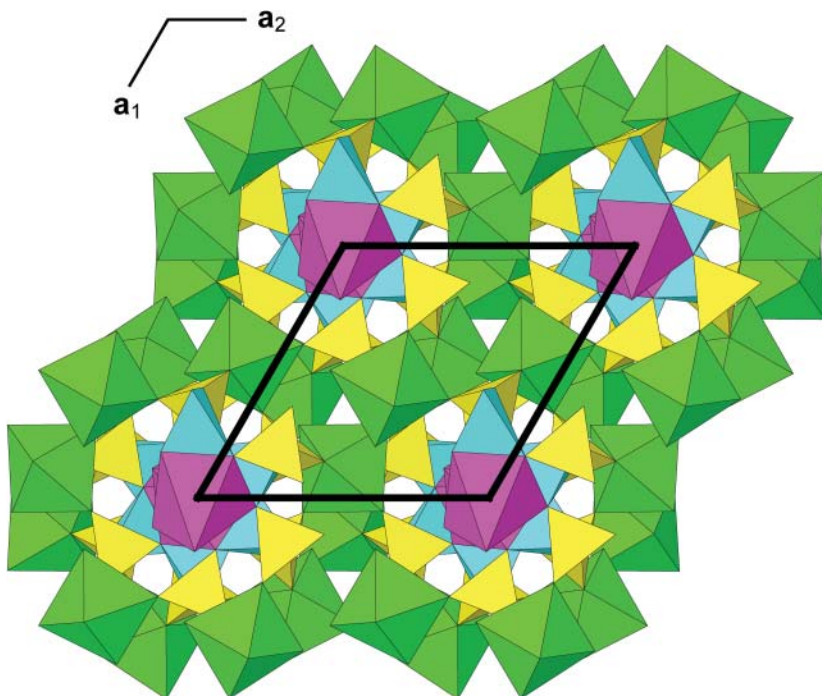


FIG. 5. The crystal structure of faheyite projected down [001]. Legend as in Figure 2; unit-cell outline marked in black.

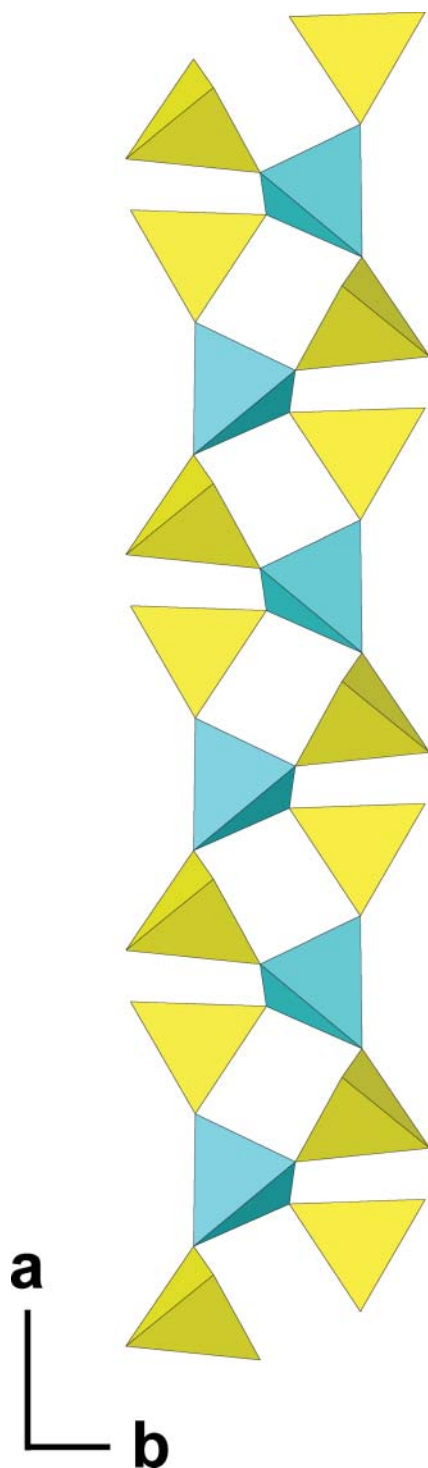


FIG. 6. The  $[\text{Be}(\text{PO}_4)(\text{PO}_3\text{OH})]$  chain in fransoletite and parafransoletite; projected onto (001).

of each  $P$  tetrahedron are shared with neighboring  $Be$  tetrahedra to form a corner-sharing  $[\text{Be}(\text{PO}_4)_2]$  chain, with  $P$  tetrahedra flanking the  $Be$  tetrahedra of the central spine in the sequence  $-P(1)/P(1)-Be-P(2)/P(2)-Be-$  (Fig. 2a). Note that faheyite has a chiral structure, with the  $[\text{Be}(\text{PO}_4)_2]$  chain twisting about the  $c$ -axis in a clockwise direction (Fig. 2b) for the refined  $P3_121$  enantiomer.

The  $Mn$  octahedron lies along the  $3_1$  screw axis within the core region of the  $[\text{Be}(\text{PO}_4)_2]$  chain, forming  $[\text{MnBe}_2(\text{PO}_4)_4]$  spires parallel to  $[001]$  (Figs. 2a, 3). These  $[\text{MnBe}_2(\text{PO}_4)_4]$  spires are wrapped by  $Fe$  octahedra that share vertices with  $P$  tetrahedra (Figs. 4, 5), and the structure shows a distinctive chemical segregation from  $Mn \rightarrow Be \rightarrow P \rightarrow Fe$  radially outward from the  $3_1$  screw axis through the origin (Fig. 5).

#### Hydrogen bonding

We were unable to reliably locate the H atoms in the final difference-Fourier map. However, from inspection of the bond valences (Table 4), it is apparent that the anions O(1) through O(8) are  $\text{O}^{2-}$ , and O(9), O(10), and O(11) are  $(\text{H}_2\text{O})$  groups. The O(1) and O(2) anions have incident bond-valence sums of  $\sim 2 \text{ vu}$  and are not likely candidates for hydrogen-bond acceptors. The anions O(3)–O(8) have incident bond-valence sums from 1.81–1.91  $\text{vu}$  and may accept a single weak hydrogen-bond. Assuming no bifurcated hydrogen-bonds, there would be a total of six hydrogen bonds originating from the three  $(\text{H}_2\text{O})$  groups [O(9), O(10), and O(11)], and six prospective hydrogen-bond acceptor anions; O(3)–O(8). However, examination of the region around each  $(\text{H}_2\text{O})$  group shows that there is no simple solution for the overall pattern of simple hydrogen bonds (*i.e.*, with respect to usual  $\text{O}_D-\text{O}_A$  distances,  $\text{O}_A-\text{O}_D-\text{O}_A$  angles, avoidance of hydrogen bonding along polyhedron edges). The more likely hydrogen-bond arrangements are given in Table 3. It is not clear whether O(6) or O(8) receives a hydrogen bond, as potential  $\text{O}_D$  anions are more than 3.3 Å away. Such distances are known to be involved in weak hydrogen bonds (Brown 1976), but in very different types of structures.

#### RELATED MINERALS

The crystal structures of fransoletite and parafransoletite (Kampf 1992) also contain beryllophosphate chains topologically identical to that found in faheyite (*cf.* Figs. 2a, 6). The  $[\text{Be}(\text{PO}_4)(\text{PO}_3\text{OH})]$  chain in fransoletite and parafransoletite is a straight chain parallel to  $[100]$ , whereas the  $[\text{Be}(\text{PO}_4)_2]$  chain in faheyite is twisted about the central  $c$ -axis.

#### ACKNOWLEDGMENTS

We thank reviewers Joel Grice and John Hughes for their comments and Associate Editor Andreas Ertl

for his comments on this paper. This work was supported by a Canada Research Chair in Crystallography and Mineralogy, Research Tools and Equipment, and Discovery Grants from the Natural Sciences and Engineering Research Council of Canada, and Canada Foundation for Innovation Grants, both to FCH.

## REFERENCES

- BROWN, I.D. (1976) Hydrogen bonding in perchloric acid hydrates. *Acta Crystallographica* **A32**, 786–792.
- BROWN, I.D. & ALTERMATT, D. (1985) Bond-valence parameters obtained from a systematic analysis of the inorganic crystal structure database. *Acta Crystallographica* **B41**, 244–247.
- BRUKER ANALYTICAL X-RAY SYSTEMS (1997) SHELXTL Reference Manual 5.1. Bruker AXS Inc., Madison, Wisconsin, United States.
- ČERNÝ, P. (2002) Mineralogy of beryllium in granitic pegmatites. *Reviews in Mineralogy and Geochemistry* **50**, 405–444.
- HAWTHORNE, F.C. & HUMINICKI, D.M.C. (2002) The crystal chemistry of beryllium. *Reviews in Mineralogy and Geochemistry* **50**, 333–403.
- HUMINICKI, D.M.C. & HAWTHORNE, F.C. (2002) The crystal chemistry of the phosphate minerals. *Reviews in Mineralogy and Geochemistry* **48**, 123–253.
- KAMPF, A.R. (1992) Beryllorphosphate chains in the structures of fransoletite, parafransoletite, and ehrlite and some general comments on beryllorphosphate linkages. *American Mineralogist* **77**, 848–856.
- LE PAGE, Y. (1988) MISSYM1.1 - a flexible new release. *Journal of Applied Crystallography* **21**, 983–984.
- LINDBERG, M.L. (1964) Mineralogical notes: Crystallography of faheyite, Sapucaia pegmatite mine, Minas Gerais, Brazil. *American Mineralogist* **49**, 395–398.
- LINDBERG, M.L. & MURATA, K.J. (1953) Faheyite, a new phosphate mineral from the Sapucaia pegmatite mine, Minas Gerais, Brazil. *American Mineralogist* **38**, 263–270.
- ROBINSON, G.W., KING, V.T., ASSELBORN, E., CURETON, F., TSCHERNICH, R., & SIELECKI, R. (1992) What's new in Minerals? *Mineralogical Record* **23**, 423–438.
- SHANNON, R.D. (1976) Revised effective ionic radii and systematic studies of interatomic distances in halides and chalcogenides. *Acta Crystallographica* **A32**, 751–767.
- SHELDRIK, G.M. (2008) A short history of SHELX. *Acta Crystallographica* **A64**, 112–122.
- VON KNORRING, O. (1985) Some mineralogical, geochemical and economic aspects of lithium pegmatites from the Karibib-Cape Cross pegmatite field in South West Africa/Namibia. *Communications of the Geological Survey of Southwest Africa/Namibia* **1**, 79–84.

Received June 3, 2014, revised manuscript accepted December 29, 2014.

